

SimCP:  $^1\text{H}$ NMR (400 MHz,  $\text{CDCl}_3$ ):  $\delta$  (ppm) 8.09 (d, 4H,  $J=7.6$  Hz), 7.86 (s, 3H), 7.67 (d, 6H,  $J=6.3$  Hz), 7.34–7.46 (m, 17H), 7.26 (d, 4H,  $J=7.3$  Hz).  $^{13}\text{C}\{^1\text{H}\}$ NMR (100 MHz,  $\text{CDCl}_3$ ):  $\delta$  (ppm) 140.4, 138.9, 136.3, 133.0, 132.8, 130.1, 128.2, 126.1, 125.5, 123.6, 120.4, 120.3, 109.7. FABMS: Calcd MW, 666.25,  $m/e=667.0$  ( $M^++1$ ). Anal. Calcd for  $\text{C}_{48}\text{H}_{34}\text{N}_2\text{Si}$ : C, 86.45; H, 5.14; N, 4.20. Found: C, 86.31; H, 5.15; N, 4.36.

Received: August 22, 2004  
Final version: October 4, 2004

- [1] M. A. Baldo, D. F. O'Brien, Y. You, A. Shoustikov, M. E. Thompson, S. R. Forrest, *Nature* **1998**, 395, 151.
- [2] M. A. Baldo, S. Lemansky, P. E. Burrows, M. E. Thompson, S. R. Forrest, *Appl. Phys. Lett.* **1999**, 76, 4.
- [3] A. Kohler, J. S. Wilson, R. H. Friend, *Adv. Mater.* **2002**, 14, 701.
- [4] S. R. Forrest, *Org. Electron.* **2003**, 4, 45.
- [5] C. W. Tang, S. A. VanSlyke, *Appl. Phys. Lett.* **1987**, 51, 913.
- [6] S. C. Stinson, *Chem. Eng. News* **2000**, 78, 22.
- [7] S. M. Kelly, *Flat Panel Displays: Advanced Organic Materials*, Royal Society of Chemistry, London **2000**.
- [8] B. Johnstone, *Technol. Rev.* **2001**, 104, 80.
- [9] O. Gelsen, *Opto & Laser Eur.* **2003**, 107, 33.
- [10] W. E. Howard, *Sci. Am.* **2004**, 290, 76.
- [11] B. W. D'Andrade, M. E. Thompson, S. R. Forrest, *Adv. Mater.* **2002**, 14, 147.
- [12] S. Tokito, T. Iijima, T. Suzuki, F. Sato, *Appl. Phys. Lett.* **2003**, 83, 2459.
- [13] B. W. D'Andrade, R. J. Holmes, S. R. Forrest, *Adv. Mater.* **2004**, 16, 624.
- [14] M. Hack, J. J. Brown, *Inf. Disp.* **2004**, 20, 12.
- [15] J. R. Sheats, *J. Mater. Res.* **2004**, 19, 1974.
- [16] M. Ikai, S. Tokito, Y. Sakamoto, T. Suzuki, Y. Taga, *Appl. Phys. Lett.* **2001**, 79, 156.
- [17] C. Adachi, M. A. Baldo, M. E. Thompson, S. R. Forrest, *J. Appl. Phys.* **2001**, 90, 5048.
- [18] J.-P. Duan, P.-P. Sun, C.-H. Cheng, *Adv. Mater.* **2002**, 15, 224.
- [19] Y.-J. Su, H.-L. Huang, C.-L. Le, C.-H. Chien, Y.-T. Tao, P.-T. Chou, S. Datta, R.-S. Liu, *Adv. Mater.* **2002**, 15, 884.
- [20] A. Tsuboyama, H. Iwawki, M. Furugori, T. Mukaide, J. Kamatani, S. Igawa, T. Moriyama, S. Miura, T. Takiguchi, S. Okada, M. Hoshino, K. Ueno, *J. Am. Chem. Soc.* **2003**, 125, 12971.
- [21] C. Adachi, R. C. Kwong, P. Djurovich, V. Adamovich, M. A. Baldo, M. E. Thompson, S. R. Forrest, *Appl. Phys. Lett.* **2001**, 79, 2082.
- [22] R. J. Holmes, S. R. Forrest, Y.-J. Tung, R. C. Kwong, J. J. Brown, S. Garon, M. E. Thompson, *Appl. Phys. Lett.* **2003**, 82, 2422.
- [23] S. Tokito, T. Iijima, Y. Suzuri, H. Kita, T. Suzuki, F. Sato, *Appl. Phys. Lett.* **2003**, 83, 569.
- [24] R. J. Holmes, B. W. D'Andrade, S. R. Forrest, X. Ren, J. Li, M. E. Thompson, *Appl. Phys. Lett.* **2003**, 83, 3818.
- [25] V. Adamovich, J. Brooks, A. Tamayo, A. M. Alexander, P. I. Djurovich, B. W. D'Andrade, C. Adachi, S. R. Forrest, M. E. Thompson, *New J. Chem.* **2002**, 26, 1171.
- [26] V. Adamovich, S. R. Cordero, P. I. Djurovich, A. Tamayo, M. E. Thompson, B. W. D'Andrade, S. R. Forrest, *Org. Electron.* **2003**, 4, 77.
- [27] T. Thoms, S. Okada, J.-P. Chen, M. Furugori, *Thin Solid Films* **2003**, 436, 264.
- [28] K. Brunner, A. van Dijken, H. Borner, J. J. A. M. Bastiaansen, N. M. M. Kiggen, B. M. W. Langeveld, *J. Am. Chem. Soc.* **2004**, 126, 6035.
- [29] S. Lamansky, P. Djurovich, D. Murphy, F. Abdel-Razzaq, R. Kwong, I. Tsyba, M. Bortz, B. Mui, R. Bau, M. E. Thompson, *Inorg. Chem.* **2001**, 40, 1704.
- [30] S. Lamansky, P. Djurovich, D. Murphy, F. Abdel-Razzaq, H.-E. Lee, C. Adachi, P. E. Burrows, S. R. Forrest, M. E. Thompson, *J. Am. Chem. Soc.* **2001**, 123, 4304.

- [31] V. V. Grushin, N. Herron, D. D. LeCloux, W. J. Marshall, V. A. Petrov, Y. Wang, *Chem. Commun.* **2001**, 1494.
- [32] T. Tsuzuki, N. Shirasawa, T. Suzuki, S. Tokito, *Adv. Mater.* **2003**, 15, 1455.
- [33] J. Li, P. I. Djurovich, B. D. Alleyne, I. Tsby, N. N. Ho, R. Bau, M. E. Thompson, *Polyhedron* **2004**, 23, 419.
- [34] P. Coppo, E. A. Plummer, L. De Cola, *Chem. Commun.* **2004**, 1774.
- [35] J. Shi, C. W. Tang, C. H. Chen, *U. S. Patent 5 645 948*, **1997**.
- [36] M. Nonoyama, *Bull. Chem. Soc. Jpn.* **1974**, 47, 767.
- [37] J. M. McManus, R. M. Herbst, *J. Org. Chem.* **1959**, 24, 1462.
- [38] S. Kubota, M. Uda, T. Nakagawa, *J. Heterocycl. Chem.* **1975**, 12, 855.
- [39] K. Funabiki, N. Noma, G. Kuzuya, M. Matsui, K. Shibata, *J. Chem. Res., Miniprint* **1999**, 1301.
- [40] L.-H. Chan, R.-H. Lee, C.-F. Hsieh, H.-C. Yeh, C.-T. Chen, *J. Am. Chem. Soc.* **2002**, 124, 6469.
- [41] S. R. Forrest, D. D. C. Bradley, M. E. Thompson, *Adv. Mater.* **2003**, 15, 1043.
- [42] G. Wyszecski, W. S. Stiles, *Color Science: Concepts and Methods, Quantitative Data and Formulae*, 2nd ed., Wiley, New York **1982**, p. 259.

## Microfabricated Deposition Nozzles for Direct-Write Assembly of Three-Dimensional Periodic Structures\*\*

By Ranjeet B. Rao, Karen L. Krafcik,  
Alfredo M. Morales, and Jennifer A. Lewis\*

Three-dimensional (3D) periodic structures fabricated from colloidal "building blocks" may find widespread technological application as advanced ceramics,<sup>[1]</sup> sensors,<sup>[2]</sup> composites,<sup>[3]</sup> tissue engineering scaffolds,<sup>[4]</sup> and photonic materials.<sup>[5]</sup> Many targeted applications require periodicity at length scales far exceeding colloidal dimensions, with lattice constants ranging from several micrometers to millimeters. Robotic deposition, a direct-write assembly technique, is capable of producing 3D periodic structures comprised of cylindrical rods.<sup>[6]</sup> Such structures are built by patterning a continuous filament that has been extruded through a cylindrical deposition nozzle. Here,

[\*] Prof. J. A. Lewis, R. B. Rao  
Department of Materials Science and Engineering  
University of Illinois at Urbana Champaign  
1304 West Green Street, Urbana, IL 61801 (USA)  
E-mail: jalewis@staff.uiuc.edu

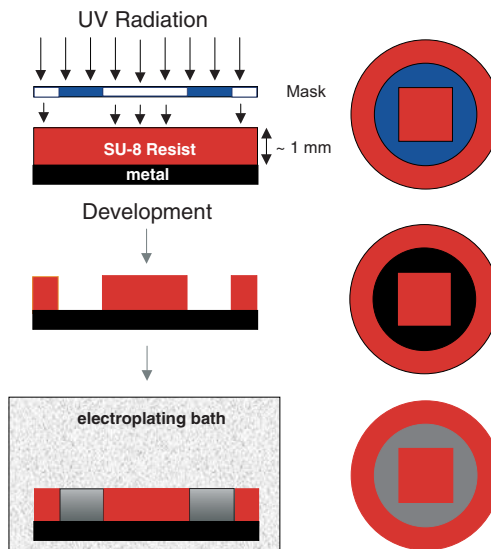
K. L. Krafcik, Dr. A. M. Morales  
Sandia National Laboratories  
7011 East Avenue, MS 94550, Livermore, CA 94550 (USA)

[\*\*] This material is based upon work supported by the National Science Foundation (Grant# CTS-0120978 and DMI-0099360) and in-kind funding from Sandia National Laboratories. R. B. Rao thanks the U.S. Department of Defense for an NDSEG research fellowship. SEM analysis was carried out in the Center for Microanalysis of Materials at the Frederick Seitz Materials Research Laboratory, University of Illinois, which is partially supported by the U.S. Department of Energy under grant DEFG02-91-ER45439.

for the first time, we describe the fabrication of 3D periodic structures comprised of non-cylindrical filaments using an approach that marries a lithographic, galvanofarming, abforming (translated as lithography, electroplating, and molding), LIGA-based technique, used to create microfabricated deposition nozzles, with direct-write assembly.

High aspect ratio micro( $\mu$ )-tips that alter deposition nozzle geometry can be fabricated by several routes, including LIGA,<sup>[7]</sup>  $\mu$ -injection molding(MIM),<sup>[8]</sup>  $\mu$ -stereolithography,<sup>[9]</sup> or  $\mu$ -electro-discharge machining( $\mu$ EDM).<sup>[10]</sup> We adapted a LIGA microgear<sup>[11]</sup> for use as a  $\mu$ -tip to demonstrate the extrusion of colloidal ink through a complex geometric orifice (Fig. 1a). UV-LIGA was then used to fabricate  $\mu$ -tips with the simplified geometries of interest (see Scheme 1). Our approach employs SU-8, a near-UV negative photoresist, which is capable of producing LIGA-like, high aspect ratio micro-parts without the need for synchrotron X-ray radiation sources.<sup>[12]</sup> The  $\mu$ -tips were formed by patterning ultrathick SU-8 photoresist using photolithography, followed by an electroplating procedure to create sub-millimeter metallic structures with precise geometrical features at a 10  $\mu$ m resolution.<sup>[13]</sup> Specifically, a Watts nickel plating bath was used to produce the hexagonal and square  $\mu$ -tips shown in Figures 1b,c. By attaching individual  $\mu$ -tips to the end of a cylindrical deposition nozzle, non-cylindrical ink filaments could be extruded during direct writing, as show in Figure 1d–f.

Concentrated colloidal gel-based inks are well suited for direct-write assembly, as previously demonstrated by Lewis and co-workers.<sup>[6,14]</sup> A colloidal ink was produced by first creating



**Scheme 1.** Schematic illustration of the micro( $\mu$ )-tip fabrication process. A thick layer (~1 mm) of SU-8 resist is spin-cast onto a metal substrate, which is illuminated with UV radiation. A mask is used to control precisely where radiation impinges on the resist, making it insoluble to the developer. A developing step is performed to remove the unexposed resist and expose areas of the underlying metal substrate. The substrate is then placed into an electroplating bath and metal is deposited upon the substrate to create the desired micro-fabricated part.

a highly concentrated suspension comprised of aluminum oxide ( $\text{Al}_2\text{O}_3$ ) particles dispersed by poly(acrylic acid) (PAA).

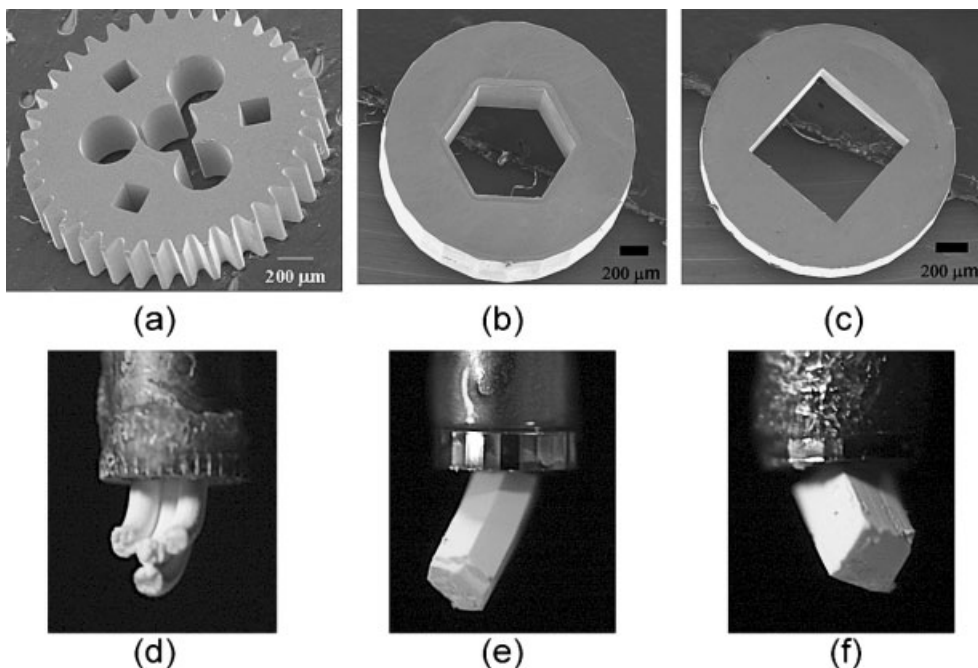


**Figure 1.** a–c) SEM images of the micro( $\mu$ )-tips: a) LIGA gear b) UV-LIGA  $\mu$ -tip with a 560  $\mu$ m vertex-to-vertex hexagonal orifice, and c) UV-LIGA  $\mu$ -tip with a 745  $\mu$ m (edge length) square orifice. d–f) Corresponding optical images of ink filaments formed by extrusion through these deposition nozzles modified with the attached  $\mu$ -tips which contain faceted side walls at their outer diameter.

PAA is an anionic polyelectrolyte with a linear backbone that contains one ionizable carboxylic acid group (COONa) per monomer unit. PAA is fully ionized at  $\sim$  pH 9 and, hence, negatively charged at the pH of interest. The desired fluid–gel transition was then induced by adding polyethyleneimine (PEI), which is a highly branched, cationic polyelectrolyte with a 1:2:1 ratio of primary, secondary, and tertiary amines. This approach differs from our earlier work, which relied on inorganic salts<sup>[15]</sup> or pH changes<sup>[14b]</sup> to trigger gelation. The current method produces inks with more uniform rheological properties by avoiding unwanted precipitation of solids from solution.

The ink rheology can be tuned to permit flow during deposition, while simultaneously promoting shape retention of the extruded filament by varying the ratio of positive  $[\text{NH}_x^+]$  to negative  $[\text{COO}^-]$  ionizable groups, as shown in Figure 2. As the  $[\text{NH}_x^+]:[\text{COO}^-]$  ratio increases, both the shear yield stress ( $\tau_y$ ) and ink elasticity ( $G'$ ) increase by orders of magnitude. Below  $\tau_y$ ,  $G'$  is independent of applied stress (i.e., the system resides in the linear viscoelastic region). Above  $\tau_y$ , interparticle bonds rupture leading to a sharp decrease in  $G'$  and apparent viscosity (see Fig. 2b), which is needed to facilitate flow. Upon exiting the nozzle, the ink returns to a quiescent state, where rapid (re)formation of interparticle bonds leads to its gelation and concurrent rise in elasticity. This solidification process ensures that the non-cylindrical filament cross-section is maintained during deposition (see Figs. 1d–f) and that the filaments can span gaps in the underlying layer(s) without deforming under their own load (see Fig. 3c).

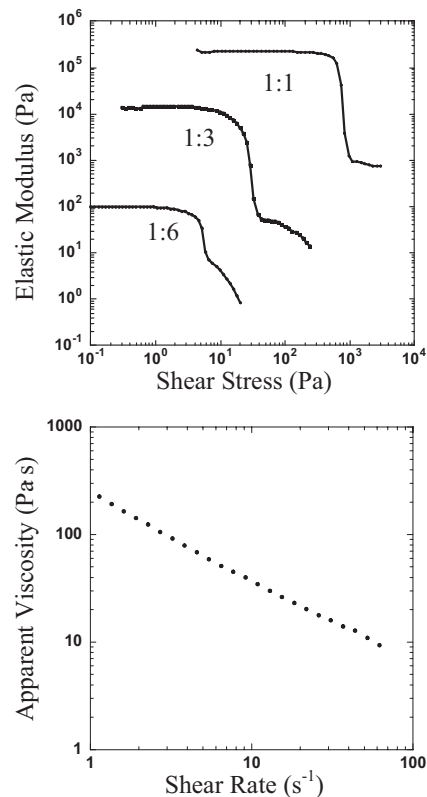


**Figure 2.** a) Log–log plot of ink elasticity as a function of applied shear stress for varying  $[\text{NH}_x^+]:[\text{COO}^-]$  ratios, and b) parent viscosity as a function of shear rate for a colloidal ink with a  $[\text{NH}_x^+]:[\text{COO}^-]$  ratio of 1:1.

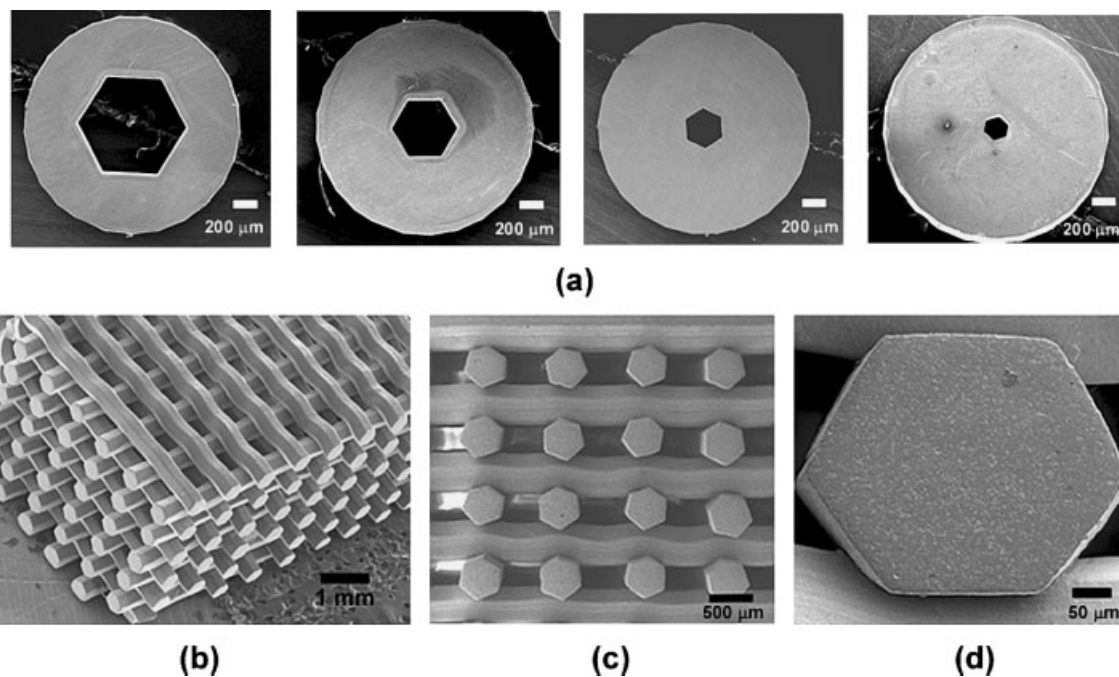


**Figure 3.** a) SEM images of hexagonal micro ( $\mu$ )-tips with vertex-to-vertex diameters of 920, 560, 360, and 170  $\mu\text{m}$  (from left to right), respectively. b–d) SEM images of 3D periodic structure (b) deposited using a 560  $\mu\text{m}$  hexagonal  $\mu$ -tip acquired at different magnifications. Note, the deposited filaments span gaps in the underlying layer(s) without significant deformation (c) and maintain their hexagonal shape (d).

Periodic structures (3D) comprised of hexagonal filaments were produced to demonstrate our fabrication capabilities. A series of hexagonal  $\mu$ -tips with vertex-to-vertex diameters of 920, 560, 360, and 170  $\mu\text{m}$ , respectively, are shown in Figure 3a. These  $\mu$ -tips possess a sharply defined orifice and vary in thickness from 200 to 500  $\mu\text{m}$  with a diameter of 1.8 mm. Three-dimensional structures were created by robotic deposition of the colloidal ink through a modified deposition nozzle (with a 560  $\mu\text{m}$  hexagonal tip attached) onto a moving  $x$ - $y$  stage yielding a (two dimensional) 2D pattern in a layerwise fashion. After a given layer is generated, the stage is incremented in the  $z$ -direction and another layer is deposited. This process is repeated until the desired 3D structure is produced. The deposition nozzle does not rotate during the patterning process; therefore, some orientation issues arise. For example, if the nozzle is correctly aligned in one layer so that the hexagonal filament is deposited with a flat face parallel to the substrate, it will be deposited with its vertex towards the substrate on the subsequent, orthogonal layer. One can observe that these spanning filaments undulate slightly along the casting direction, as both their edges and vertex are clearly visible (see Figs. 3b,c). However, the cross-section view of the 3D structure reveals that the filaments exhibit little deformation, as they span gaps in the underlying layer(s) (Fig. 3c). In addition, it is clear that the filament cross-section (Fig. 3d) maintains its hexagonal shape after assembly, drying, and densification of the structure at elevated temperatures.

The rate at which the ink solidifies after it exits the deposition nozzle strongly influences the shape evolution of the as-deposited features. In the absence of (re)gelation, the filament would remain viscous and evolve to a cylindrical shape driven by surface tension. One can estimate the characteristic time scale required for viscous flow using the model developed by Kuiken ( $t^*$ ):<sup>[16]</sup>

$$t^* = \frac{l\eta}{\gamma} \quad (1)$$

where perturbations from a circular cross-section (i.e., constant curvature) are restored within  $10t^*$ ,  $l$  is a characteristic length scale ( $\sim 0.5$  mm, the approximate tip opening),  $\eta$  is the dynamic viscosity, and  $\gamma$  is the surface tension (measured value of 50  $\text{mN m}^{-1}$ ). Using Equation 1, we find that surface-tension-driven flow would occur quickly ( $\sim$  few seconds) for ink filaments possessing a high shear viscosity of 40 Pa s in the quiescent state. This value corresponds to the apparent ink viscosity observed (see Fig. 2b) at a shear rate of 10  $\text{s}^{-1}$ , which is the maximum rate predicted at the nozzle wall under a no-slip boundary condition.<sup>[14b]</sup> This analysis highlights one important advantage of using colloidal-gel-based inks for direct-write assembly of non-cylindrical features, since rapid (re)gelation suppresses viscous flow thereby preserving the desired extruded shape.

Smay et al.<sup>[14b]</sup> calculated the minimum ink elasticity required to produce spanning filaments within a 3D periodic structure comprised of cylindrical filaments (or rods). Using a

simply supported, elastic beam model, the minimum elastic modulus  $G'$  required to have a midpoint deflection of no greater than 5 % of the rod diameter is given by:

$$G' \geq 1.4 \gamma s^4 D \quad (2)$$

where  $\gamma$  is the specific weight of the ink ( $= \rho_{\text{gel}} \cdot g_0$ ),  $g_0$  is the gravitational constant,  $D$  is the rod diameter, and  $s$  is the normalized span distance ( $= L/D$ ). If the cross-section of the beam is hexagonal rather than circular, the moment of inertia changes, resulting in the following relation:

$$G' \geq 1.66 \gamma s^4 D \quad (3)$$

with  $D$  now being the vertex-to-vertex diameter of the hexagon. Hexagonal filaments therefore require more stringent demands on ink elasticity than their cylindrical counterparts. For square filaments, the coefficient is increased even further, to 2.94, where  $D$  is taken to be the corner-to-corner distance. During deposition, only the volume surrounding the central axis of the filament remains gelled. For inks with similar rheological properties flowing through a cylindrical nozzle, the gelled core region has an initial radius about 10 % of the filament radius immediately upon exiting the nozzle.<sup>[14b]</sup> If we assume a similar core-shell architecture, then the ink stiffness required to produce spanning filaments increases by a factor of  $10^4$ , to approximately  $3.9 \times 10^5$  Pa. Note, this  $G'$  value decreases with decreasing tip size. Since the colloidal ink utilized here had a  $G'$  value of approximately  $5 \times 10^5$  Pa, the hexagonal filaments can readily span gaps in the underlying layers with minimal deformation (see Fig. 3c).

In summary, we have demonstrated the direct-write assembly of 3D periodic structures with non-cylindrical features. A LIGA-based microfabrication technique was used to create  $\mu$ -tips of the desired geometry. Colloidal gel-based inks enabled the deposited filaments to maintain their shape and span gaps in the underlying layer(s) without significant deformation. By coupling these assembly routes, we have expanded the palette of 3D periodic structures that can be produced. These novel 3D architectures may find potential application as structural ceramics, filters, and catalyst supports, or as a skeletal framework in composites. In addition to altering the filament geometry formed during direct-write assembly, these  $\mu$ -tips may also be utilized as die tooling in other extrusion-based microfabrication techniques.

## Experimental

$\text{Al}_2\text{O}_3$  powder (AKP-15, Sumitomo Chemical Co., New York) with a specific surface area of 3.9  $\text{m}^2 \text{g}^{-1}$ , density of 3.97  $\text{g cm}^{-3}$ , and mean particle size of 0.7  $\mu\text{m}$ , and  $\text{ZrO}_2$  powder (3Y-TZ, Tosoh Corp, Tokyo, Japan) with a specific surface area of 14.3  $\text{m}^2 \text{g}^{-1}$ , density of 5.89  $\text{g cm}^{-3}$ , and mean particle size of 0.28  $\mu\text{m}$  served as the colloidal phase. Poly(acrylic acid) sodium salt (Darvan 821A, R.T. Vanderbilt Co, Inc., Norwalk, CT), supplied as a 40 % aqueous solution, served

as a dispersant for the colloidal particles. Stable colloidal suspensions (30 vol.-%) were produced by adding the appropriate amounts of dispersant and powder (95:5 volumetric ratio of  $\text{Al}_2\text{O}_3/\text{ZrO}_2$ ) to deionized water. The suspensions were then vigorously agitated for 1 hour to ensure their homogeneity and then centrifuged at 2500 rpm for 45 min. After centrifuging, the supernatant was removed to increase the solids loading to approximately 54 vol.-%. 5 mg of methylcellulose (Methocel F4M, Dow Chemical Co., Midland, MI) per mL of ceramic was added as a viscousifying agent. Gelation was induced by adding polyethyleneimine (PEI, Polysciences, Warrington, PA), with an average molecular weight of  $600 \text{ g mol}^{-1}$ . 6.3  $\mu\text{L}$  PEI solution (40 wt.-%) was added per mL of powder to induce gelation. The final solids loading of the colloidal ink was approximately 52 vol.-%.

Two different sets of micro( $\mu$ )-tip geometries, one hexagonal and one square, were electroformed in molds created by patterning a thick photoresist formulation (DKS) with a broadband UV aligner. The photoresist consisted of 69 % of solids SU8 R 50 resin (MicroChem), 3 % of solids PAG (phenyl-*p*-octyloxyphenyl-iodoniumhexafluoroantimonate from GE Silicones) photo acid generator, 10 % TIBA (triisobutylamine)/PAG by mole. The TIBA is a 10 % solution by mass in PGMEA (Shipley). For each set of molds, a 1.2 mm thick Si wafer was first metallized with 750 Å of Ti followed by 4000 Å of copper, 750 Å of Ti, plus 1000 Å  $\text{SiO}_2$ . A thick DKS layer (450  $\mu\text{m}$ ) was applied to the wafer in two spin-coats. For the first spin-coat, approximately 4 mL of DKS were poured onto the center of the metallized wafer, spun at 640 rpm for 15 s, and baked on a hot plate at 95 °C for 25 min. For the second spin-coat, approximately 4 mL of DKS were poured onto the center of the metallized wafer, spun at 640 rpm for 15 s, and baked on a hot plate at 95 °C for 35 min. The edge bead was then removed by squirting acetone on the edge of the wafer while spinning the wafer at 600 rpm. In order to relieve internal stresses in the DKS coat, a post apply bake was carried out by heating the wafer on a hot plate from room temperature to 95 °C at a rate of  $45^\circ\text{C h}^{-1}$ , holding at temperature for 4 h, and then cooling back down to room temperature at a rate of  $60^\circ\text{C h}^{-1}$ .

The wafer was then exposed with a Karl Suss MA6 broadband UV aligner under soft contact to a total dose of  $8.096 \text{ mJ cm}^{-2}$  measured at 365 nm. A post-exposure bake was carried out by heating on a hot plate from room temperature to 85 °C at  $60^\circ\text{C h}^{-1}$ , holding at temperature for 1 h, and then cooling back down to room temperature at a rate of  $60^\circ\text{C h}^{-1}$ . The wafer was then immersion developed in a crystallization dish of PGMEA based SU8 developer (MicroChem, Newton, MA, USA) for approximately 1.7 h.

A copper layer was deposited into the molds from a copper sulfate bath at  $15 \text{ mA cm}^{-2}$  for 20 min. This layer acts as both a plating base and as a release layer for the final removal of the plated microparts. The molds were then placed in a Watts-nickel electroplating bath with saccharin as a stress reliever [17] and a 200  $\mu\text{m}$  thick layer of nickel was electroformed at  $15 \text{ mA cm}^{-2}$ . After plating, the bulk of the DKS was fractured off the wafer by thermally cycling the wafer repeatedly from room temperature to 77 K in a liquid nitrogen bath. The nozzles were then released by etching away the underlying copper in an etch consisting of one part by volume of DI water, one part by volume of aqueous ammonium hydroxide, and one part by volume of 3 % aqueous hydrogen peroxide. The large plugs of DKS in the orifices of larger nozzles were removed by heating at 80 °C in saturated aqueous KOH. The smaller plugs of DKS were manually extracted with fine point tweezers.

Direct-write assembly was carried out using a robotic deposition apparatus (JL2000, Robocasting Enterprises, Inc., Albuquerque, NM). The 3-axis motion of the *x*-*y* and *z*-stages was independently controlled by a custom-designed, computer-aided program (RoboCAD 3.2, 3D Inks, LLC, Stillwater, OK) that allowed for the construction of complex, 3D architectures in a layerwise deposition scheme. The lattice structures produced consisted of a linear array of rods aligned with the *x*- or *y*-axis such that their orientation was orthogonal to the previous layer, with rod spacing equal to the width of the rods. The ink was housed in a syringe (barrel diameter 8 mm, Bec-

ton Dickinson Inc., Franklin Lakes, NJ) and deposited through a stainless steel nozzle (inner diameter  $D = 1.37 \text{ mm}$ , EFD Inc., East Providence RI) modified with a  $\mu$ -tip to alter its cross-sectional shape. Specifically, the  $\mu$ -tips were attached to the end of a stainless steel cylindrical nozzle using a cyanoacrylate adhesive (QuickTite, Manco, Inc., Avon, OH). The flow rate through the modified deposition nozzle was adjusted to maintain a constant *x*-*y* table speed of  $2 \text{ mm s}^{-1}$ . The deposition process was carried out under a non-wetting oil to prevent drying during assembly.

After fabrication and drying, the 3D periodic structures were sintered at 1600 °C for 2.5 h in air. The structures were sectioned using a low speed diamond saw (Buehler ISOMET, Buehler Ltd., Lake Bluff, IL). SEM images were acquired using either a Zeiss DSM 960 (Carl Zeiss Inc., Oberkochen Germany) or JEOL 6060LV (JEOL-USA Inc., Peabody, MA) scanning electron microscope after sputtering the structures with gold for 45 s (Emitech K575 Sputter Coater, Emitech Ltd., Ashford Kent, UK) prior to imaging.

Received: April 5, 2004  
Final version: June 25, 2004

- [1] J. A. Lewis, *J. Am. Ceram. Soc.* **2000**, *83*, 2341.
- [2] a) M. Allahverdi, S. C. Danforth, M. Jafari, A. Safari, *J. Eur. Ceram. Soc.* **2001**, *21*, 1485. b) J. F. Tressler, S. Alkoy, A. Dogan, R. E. Newnham, *Composites Part A* **1999**, *30*, 477.
- [3] a) A. Bandyopadhyay, *Adv. Eng. Mater.* **1999**, *1*, 199. b) J. E. Smay, J. Cesarano, B. A. Tuttle, J. A. Lewis, *J. Appl. Phys.* **2002**, *92*, 6119. c) R. Soundararajan, G. Kuhn, R. Atisivan, S. Bose, A. Bandyopadhyay, *J. Am. Ceram. Soc.* **2001**, *84*, 509.
- [4] a) Y. Zhang, M. Zhang, *J. Biomed. Mater. Res.* **2002**, *61*, 1. b) T.-M. G. Chu, J. W. Hallowran, S. J. Hollister, S. E. Feinberg, *J. Mater. Sci. Mater. Med.* **2001**, *12*, 471.
- [5] a) S. H. Im, Y. T. Lim, D. J. Suh, O. O. Park, *Adv. Mater.* **2002**, *14*, 1367. b) Y. A. Vlasov, X.-Z. Bo, J. C. Sturm, D. J. Norris, *Nature* **2001**, *414*, 289.
- [6] a) J. Ceserano, III, P. Calvert, *US Patent 6027326*, **2000**. b) J. E. Smay, G. M. Gratson, R. F. Shepherd, J. Cesarano, J. A. Lewis, *Adv. Mater.* **2002**, *14*, 1279.
- [7] E. W. Becker, W. Ehrfeld, P. Haggmann, A. Maner, D. Munchmeyer, *Microelectron. Eng.* **1986**, *4*, 35.
- [8] a) Z. Y. Liu, N. H. Loh, S. B. Tor, K. A. Khor, Y. Murakoshi, R. Maeda, T. Shimuzu, *J. Mater. Process. Technol.* **2002**, *127*, 165. b) R. Ruprecht, T. Gietzelt, K. Muller, V. Piotter, J. Hausselt, *Microsyst. Technol.* **2002**, *8*, 351.
- [9] a) P. G. Conrad, P. T. Nishimura, A. Damian, B. J. Schwartz, D. Wu, N. Fang, X. Zhang, M. J. Roberts, K. J. Shea, *Adv. Mater.* **2003**, *15*, 1541. b) C. Provin, S. Monneret, H. Le Gall, S. Corbel, *Adv. Mater.* **2003**, *15*, 994.
- [10] G. L. Benavides, L. F. Bieg, M. P. Saavedra, E. A. Bryce, *Microsyst. Technol.* **2002**, *8*, 395.
- [11] J. Hruby, *MRS Bull.* **2001**, *26*, 337.
- [12] J. M. Shaw, J. D. Gelorme, N. C. LaBiana, W. E. Conley, S. J. Holmes, *IBM J. Res. Dev.* **1997**, *41*, 81.
- [13] a) P. M. Dentinger, K. L. Krafcik, K. L. Simison, R. P. Janek, J. Hachman, *Microelectron. Eng.* **2002**, *61–62*, 1001. b) L. A. Domeier, M. Gonzales, J. Hachman, J. M. Hruby, R. Janek, A. M. Morales, *Microsyst. Technol.* **2002**, *8*, 78.
- [14] a) J. A. Lewis, *Curr. Opin. Solid State Mater. Sci.* **2002**, *6*, 245. b) J. E. Smay, J. Cesarano, J. A. Lewis, *Langmuir* **2002**, *18*, 5429.
- [15] Q. Li, J. A. Lewis, *Adv. Mater.* **2003**, *15*, 1639.
- [16] H. K. Kuiken, *J. Fluid Mech.* **1990**, *214*.
- [17] F. A. Lowenheim, in *Electroplating*, McGraw-Hill, Inc., New York **1978**.